

REE and Y enrichment in peralkaline felsic rocks of the Siwana region, Rajasthan, northwestern India

Suresh Kumar^{1,*}, Vivek V. Kumar¹, Shishir Bhardwaj¹, Rohit Sharma² and Kiran J. Mishra¹

¹Geological Survey of India, Western Region, Jaipur 302 017, India

²Geological Survey of India, Northern Region, Jammu 180 006, India

In the modern world, rare earth elements (REE) and yttrium (Y) dominate the development of high-end electronic equipment and green energy technologies. The global economic deposits of REE and Y are primarily associated with alkaline and peralkaline igneous rocks. The REE deposit of the Siwana ring complex, Rajasthan, India, is entirely composed of peralkaline igneous rocks. This complex is made up of REE and Y-enriched (both LREE and HREE) peralkaline granite, rhyolite and its younger felsic intrusives such as rhyolite, microgranite, aplite and felsite dykes. We present a study of the REE and Y potential of granites, volcanic rocks and felsic dykes from 17 quarries in the Siwana area. Monazite, zircon and apatite were the primary (magmatic) REE-bearing phases identified under a microscope. The late/post-magmatic replacement in granite is evident as coarsening of perthite lamellae, pseudomorphic replacement of alkali feldspar grains by aegirine, replacement of aenigmatite by aegirine, etc. The granites, volcanic rocks and dykes show significant enrichment of REE + Y and other trace elements (Sn, Hf and U). A total of 20 rock samples were analysed using inductively coupled plasma mass spectrometry, which indicated significant REE + Y values ranging between 1061.22 and 9088.62 ppm, with an average of 2361.89 ppm. This includes LREE (707.42–5743.83 ppm, avg. 2080.40 ppm) and HREE (135.77–1422.23 ppm, avg. 402.41 ppm) Hf up to 425.55 ppm. Totally five samples from a soil profile were also analysed, yielding REE + Y values between 223.39 and 3175.75 ppm, with an average of 1714.51 ppm. The ion adsorption clay horizon developed within the soil profile showed a maximum REE + Y value of 3175.75 ppm.

Keywords: Alkaline granite, igneous rocks, rare earth elements, soil profile, yttrium.

RARE earth elements (REE) and certain typically associated elements scandium and yttrium (Y) regulate modern-world technology due to their unique magnetic, catalytic and

phosphorescent properties. In the contemporary decades, REE deposits have been a prime target for India's mineral exploration endeavours, which may lead to the development of green energy and cutting-edge technologies in the country. About 13.07 million tonnes (mt) *in situ* monazite (containing ~55–60% total REE oxide) resource occurring in the coastal beach placer sands in parts of Kerala, Tamil Nadu, Odisha, Andhra Pradesh, Maharashtra, Gujarat, and in the inland placers in parts of Jharkhand, West Bengal and Tamil Nadu was considered to be the only exploitable REE reserve of India in the past decades. Significant resources of REE and associated rare metals like niobium have been established in northwestern India in recent times¹. The highly valued REEs are dysprosium and terbium used in REE permanent magnets, which are not available in extractable quantities in the Indian reserves already under exploitation¹. Based on this critical fact and recent discoveries of potential HREE reserves in peralkaline intrusive complexes and their weathering products in China, Russia and Canada, there has been a paradigm shift in the targeted host rocks for REE in the Indian subcontinent^{2,3}.

The Siwana Ring Complex (SRC) of the Malani igneous suite (MIS) of the Neoproterozoic peralkaline felsic magmatism in northwestern India hosts significant REE mineralization^{4–7}. Previous REE explorations in SRC peralkaline rocks have revealed an abnormally high concentration of REE, and Rb, Ba, Sr, K, Zr and Nb in the Siner granites and microgranites^{8–10}, anomalous total REE values ranging from the 428 to 3719 ppm from the northern part of SRC^{8,9}, total REE up to 3.4% associated with Zr up to 9944 ppm, Nb up to 1385 ppm, Th up to 571 ppm and U up to 169.25 ppm in felsite dykes of the Phulan area^{11,12}, and total REE up to 2.04 wt% in Gudanal (east), 2.23 wt% in Gudanal (west), 2.15 wt% in Meli and 2.5 wt% in Bhatikhera¹³.

This study reports significant HREE and Y concentration in granites, rhyolites and felsic dykes of the Siwana area. The study seeks to explicate the mineralogical, geochemical and genetic aspects of mineralization based on field relations, petrography, detailed geochemical analysis and electron probe microanalyzer (EPMA) studies.

*For correspondence. (e-mail: sureshgeolbhu@gmail.com)

Geological setting

The term 'Malani' is strictly used to describe rocks of the Neoproterozoic polyphase igneous activity that occurred roughly between 830 and 680 Ma, the age range representing the gap between the Sirohi Group of Delhi's and the Marwar Supergroup^{14,15}. MIS unconformably overlies the Mesoproterozoics of the Delhi Super Group¹⁶. Based on field relationship, mode and type of magmatism, texture and composition, MIS has been divided into three phases of magmatic activity. The first phase commenced with the eruption of basic flows, pyroclastic flows and voluminous outpouring of felsic to intermediate lava flows. The eruption culminated with ash-bed deposition. The second phase experienced the intrusion of granitoids as plutons, ring dykes, bosses and plugs within the extrusive phase. The third phase represented felsic dyke swarms and sills within the earlier two phases^{17–24}. SRC, a part of MIS, has a diameter of about 25 km and is located in the eastern part of the Barmer district, Rajasthan, forming a ring dyke structure^{25,26} (Figure 1). Three stages of peralkaline granite activity are identified in SRC, beginning with the intrusion of medium-to-coarse-grained granite followed by voluminous homophonous coarse-grained to pegmatoidal leucogranite. The third phase is marked by the intrusion of granite porphyry and microgranite dykes with minor rhyolite dykes and quartz veins¹³. The study area encompasses the central and southern portions of SRC that are dominated by peralkaline granite with its sub-alkaline to peralkaline volcanic

equivalents and later dykes of rhyolite, microgranite, aplite and felsite. The granites are exposed mostly in the centre of SRC. These intrusives are dominated by grey-coloured, medium- to coarse-grained granite and pink-coloured, coarse-grained alkali feldspar granite. The intrusive relationship of the granites with volcanic rocks is well-exposed in the Mokalsar and Ludrara villages of Barmer district.

Methodology

Petrographic investigation of the polished thin sections of granite and rhyolite collected from the quarries was carried out using an optical microscope (Olympus BX-51, Japan). Totally 25 samples were analysed for REE and Y, with all precautions to avoid contamination. Powdered samples of granite, rhyolite, felsic dyke and soil/clay were pelletized and analysed using ICP-MS (Varian 820-MS system, Australia) at the Chemical division, Geological Survey of India (GSI), Western Region, Jaipur, Rajasthan. The ~200 thoroughly homogenized mesh samples were weighed and mixed with lithium metaborate and lithium tetraborate flux in platinum crucibles. The solid mixture was then fused at 1050°C for 1 h to ensure complete fusion of the matrix, including the refractory elements. The fused mass was brought into a solution using nitric acid and indium as the internal standard and aspirated using the ICP-MS instrument. Backscattered electron (BSE) microscopic images of REE phases and major silicate minerals were obtained employing electron microprobe microanalysis (CAMECA SX-100, France) at the EPMA lab, GSI, Faridabad. To identify the main silicate minerals and REE-bearing mineral phases, as well as to ascertain their morphological traits and mineral composition, thin polished sections were examined. Four spectrometers and an EDS detector were part of the electron microprobe equipment. Accelerating voltage of 20 KV, current of 30 nA and peak counting time of 30 sec for all elements were used to maintain the analytical conditions. The analysis was performed using 1 µm beam size. All the natural standards were used for the calibration of the instrument. The following standard materials were used to analyse the REE minerals: CaF₂ (FKα), albite (NaKα), MgO (MgKα), Al₂O₃ (AlKα), wollastonite (SiKα, CaKα), apatite (PKα), orthoclase (KKα), TiO₂ (TiKα), rhodonite (MnKα), Fe₂O₃ (FeKα), zircon (ZrLα), SrSO₄ (SrLα), YAG (YLα), Nb (NbLα), barite (BaLα), La glass (LaLα), Pr glass (PrLβ), Nd glass (NdLβ), Sm glass (SmLβ), Gd glass (GdLβ), Dy glass (DyLβ), Ta (TaMα), Th glass (ThMα), U glass (UMβ) and Ce glass (CeLα). The following spectrometer parameters were used for the analysis: Sp4 TAP, Sp4 TAP, Sp4 TAP, Sp4 TAP, Sp1 PET, Sp3 LPET, Sp1 PET, Sp1 PET, Sp2 LIF, Sp2 LIF, Sp1 PET, Sp1 PET, Sp1 PET, Sp1 PET, Sp2 LIF, Sp2 LIF, Sp2 LIF, Sp2 LIF, Sp2 LIF, Sp2 LIF, Sp2 LIF, Sp4 TAP, Sp3 LPET,

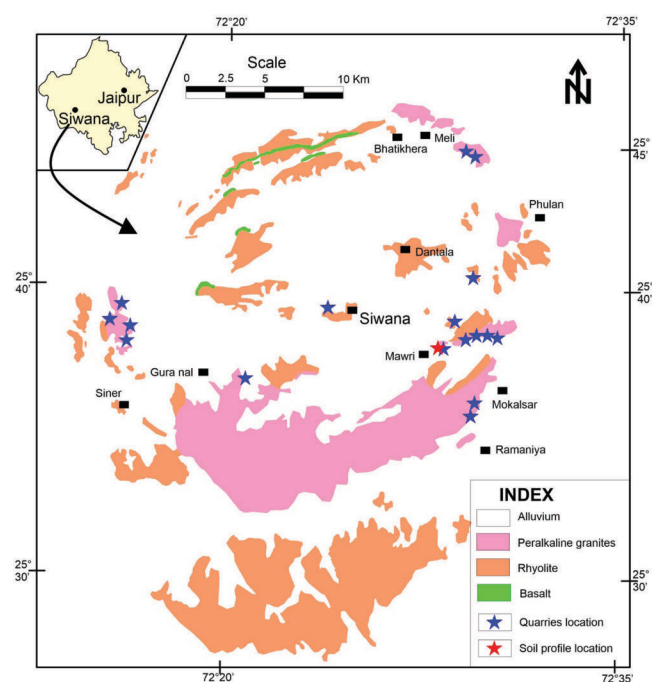


Figure 1. Geological map of the Siwana Ring Complex, Rajasthan, India, showing the exposure of felsic and basic volcanics with intrusive of peralkaline granite and location of quarries (modified after Bhushan and Somani¹³).

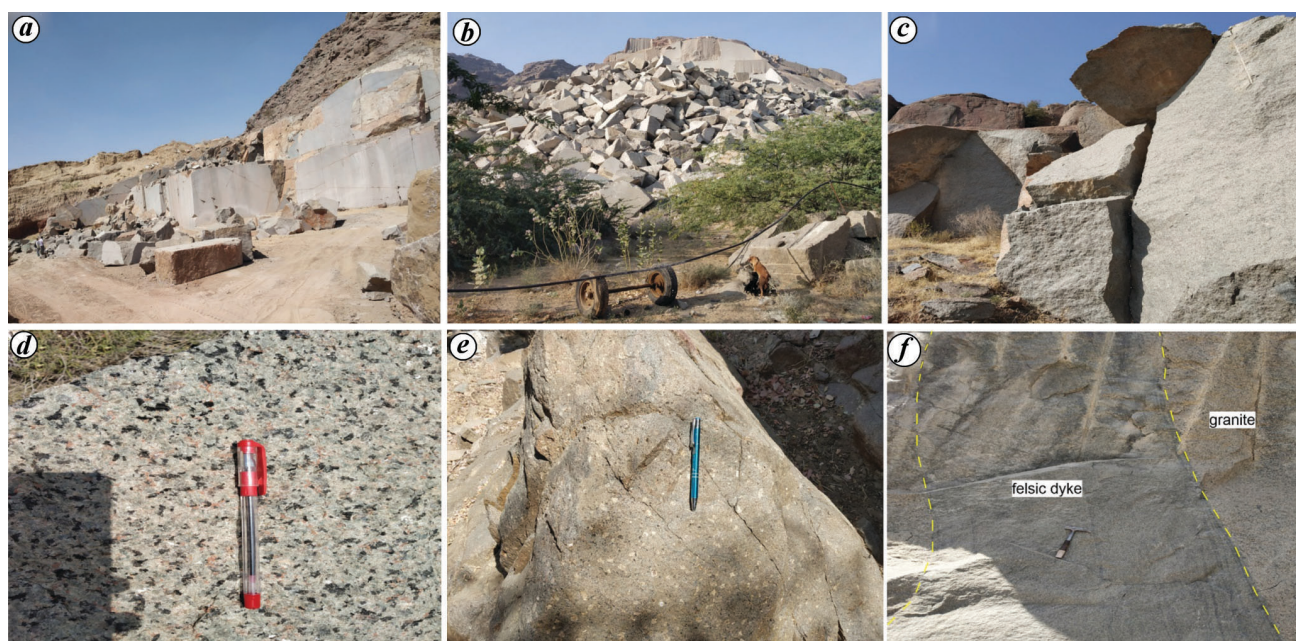


Figure 2. Field photographs showing (a–c) quarries of REE and Y-enriched granite mined out as building stones, (d) granite, (e) rhyolite and (f) felsic dyke exposed in a quarry section of the Siwana region.

Sp3 LPET, Sp2 LIF. A ZAF correction process was used to reduce the amount of data.

Results

Field relations and petrochemistry

Altogether, 17 quarry sections were explored for REE+Y potential (Figure 2a–c). Felsic rocks, viz. Peralkaline granite, rhyolite and their younger derivative felsic dykes are the dominant litho units in the southern part of SRC (Figure 1). These granites are medium- to coarse-grained and relatively equigranular. Alkali feldspar, quartz, aegirine and arfvedsonite are the most abundant minerals in the granite (Figure 2d). The rhyolite porphyry exhibited granophyric and flow texture. An aphanitic groundmass of volcanic glass, aegirine and arfvedsonite has globular quartz and euhedral feldspar phenocrysts (Figure 2e). Vesicles in these volcanic rocks are filled by secondary calcite and quartz. Felsic dykes are the latest intrusive phases into volcanic rocks and peralkaline granites of the Siwana area (Figure 2f). They occur in the thickness range 20 cm to 3 m with consistent surface extension up to 600 m, striking EW, NS and NW–SE directions. They are fine-grained, pinkish and greenish-grey-coloured with mineralogy similar to peralkaline granites and volcanic rocks.

Petrography and EPMA studies

The studied granite samples from the quarries exhibited hypidiomorphic texture and were composed essentially of alkali feldspar (quartz (40–45 in vol%), albite/oligoclase

(20–25 in vol%), aegirine (15–20 in vol%), orthoclase (10–15 in vol%), and arfvedsonite (10–15 in vol%)). The accessory phases were zircon, rutile and magnetite (Figure 3a and d). Perthite (exsolution texture) was also commonly seen in granite (Figure 3b) due to intimate intergrowth of albite within K-feldspar, indicating non-isochemical replacement. Monazite, zircon and apatite were identified as the primary (magmatic) REE-bearing phases under a microscope. The late/post-magmatic replacement in granite is evident under the microscope as coarsening of perthite lamellae, pseudomorphic replacement of alkali feldspar grains by aegirine, and replacement of aenigmatite by aegirine (Figure 3g–i). This late/post-magmatic replacement may have played a significant role in the remobilization of REE and their redistribution in the form of tiny secondary mineral phases. The silicate minerals have straight, regular grain boundaries and range in size from big euhedral to tiny anhedral crystals. Consequently, a continuous size gradation indicates that they crystallized at various depths. REE-bearing mineral phases such as monazite, zircon, xenotime and apatite occupy the intercumulus area. A few coarse K-feldspar grains altered into sericite along the grain boundary, suggesting a low degree of post-magmatic alteration (Figure 3a). Rhyolite exhibited porphyritic texture, and porphyroclast of K-feldspar and some aegirine grains were embedded within a fine-grained groundmass similar to granite (Figure 3c). Various REE mineral phases, including monazite, zircon and bastnaesite, were observed to occur in groups hosted in the alkali feldspar and quartz groundmass. Monazite and zircon, which form large euhedral phenocrysts, were the predominant REE minerals (Figure 3e and f). Along the grain boundaries of aegirine–arfvedsonite, zircon was found as coexisting intergranular blebs

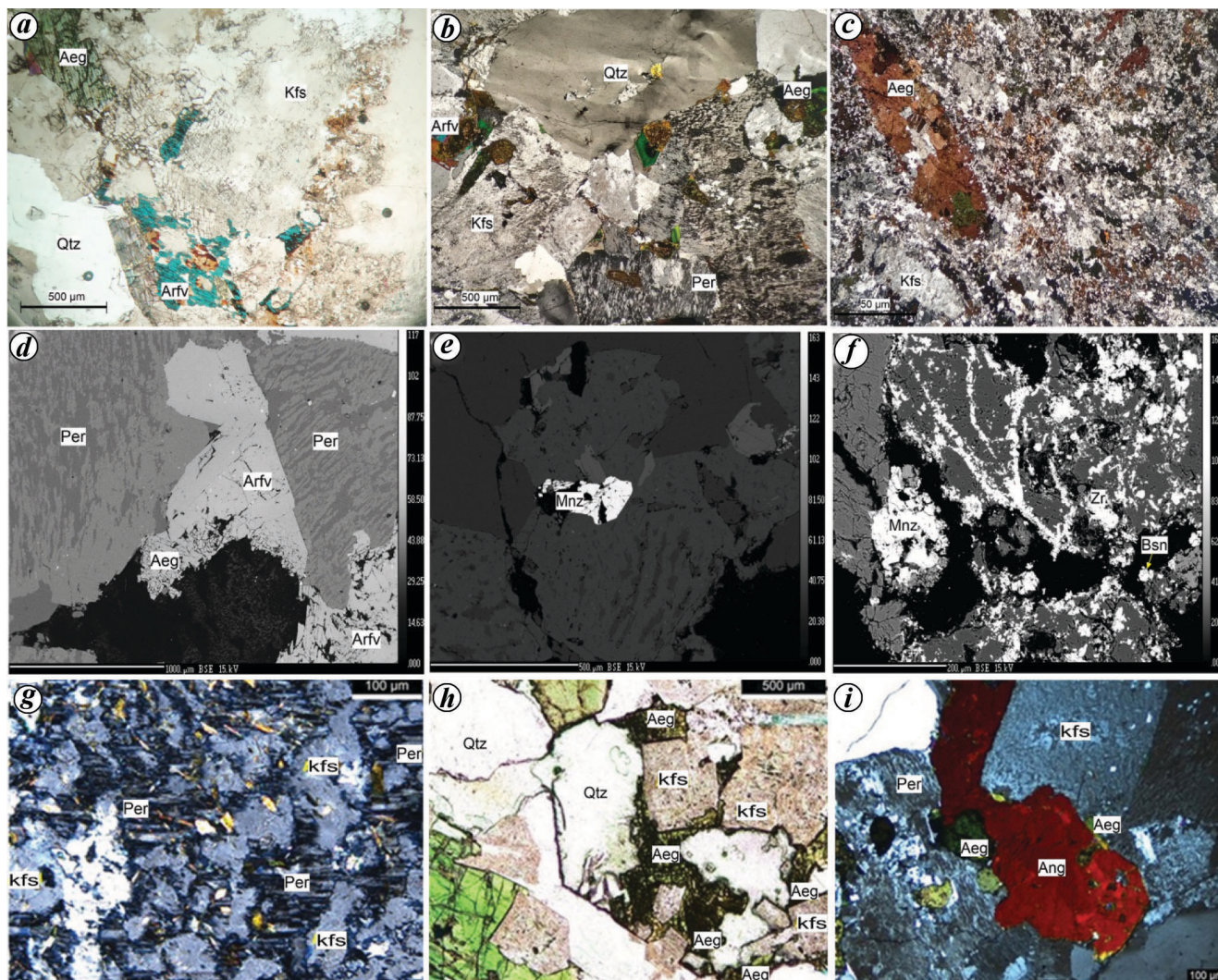


Figure 3. Petrographic study of REE and Y-enriched granite and rhyolite samples mined out as building stones. *a, b*, Coarse-grained granite showing hypidiomorphic and perthite texture (cross-polarized light). *c*, Rhyolite porphyry showing clasts of K-feldspar and aegirine embedded in fine-grained groundmass. *d–f*, Backscattered electron microscopic images of aegirine–arfvedsonite granite associated with REE-bearing minerals. *g*, Coarsening of braided perthite to patch perthite in granite. *h*, Pseudomorphic replacement of alkali feldspar by aegirine in granite. *i*, Aenigmatite replaced by aegirine in granite. (Aeg, Aegirine; Arfv, Arfvedsonite; Qtz, Quartz; Kfs, K-feldspar; Per, Perthite; Mnz, Monazite; Zr, Zircon; Bsn, Bastnaesite and Ang, Aenigmatite).

as well as veinlets (Figure 3 *e*). Bastnaesite was found to be small, separate grains (Figure 3 *f*).

The major silicate and REE minerals were characterized using EPMA and BSE imaging. Aegirine, arfvedsonite, quartz, albite and orthoclase were the major silicate minerals. REE-phosphate (monazite) and REE-carbonate (bastnaesite) were the most common REE minerals found in the studied samples (Table 1). Moreover, grains of REE-bearing zircon were also found during analysis (Figure 3 *d–f*).

Soil profile study

Considering the worldwide scenario of REE-bearing granitoids, REEs are supplied to the soil profile during the

weathering process. Enrichment or depletion of REE occurs because these elements are mobile and are fractionated during weathering²⁷. When released from the primary rocks, REEs are either lost into the soil solution from the weathering profile or incorporated into secondary minerals^{28–30}. REE behaviour in surface soils is closely related to interactions with secondary minerals, especially geochemically active secondary minerals such as Fe, Al and Mn oxides^{31,32}. Exploring the distribution and geochemical properties of REE, especially the common ones like Ce and Eu, helps deduce the evolution of the earth's surface environment^{33,34}. The relative enrichment of REE in the weathering products in relation to the bedrock is pronounced in horizon B³⁵. REE occurs in the soil profile as weakly adsorbed ions and bound with Mn, Fe-oxides,

especially Ce³⁶. In this respect, the REE and Y potential of a soil profile exposed in one of the quarry sections near Mawri village was studied (Figure 4). The profile is made up of sandy soil (3 m), sandy soil with loose granite fragments (2 m), loose unconsolidated material (5 m), oxidized zone (1 m), clay horizon (0.5 m) and granite boulders from top to bottom. The anomalous concentration of REE and Y was detected in five samples collected from top to bottom of the profile. The vertical distribution of REE and Y indicates a progressive depletion in REE concentration from bottom to top. The clay horizon has the highest REE + Y concentration (3175.75 ppm) with an encouraging LREE/HREE ratio of 4.48:1 against the global LREE/HREE ratio of 18:1 in already produced and technically accessed resources³⁷. The chondrite-normalized REE pattern of the soil profile from the quarry section reflects a strong negative Eu anomaly and a relatively weak negative Ce anomaly. This pertinent similarity of the REE pattern of the studied soil profile samples with the bedrock samples suggests very low mobility of REE during the weathering process.

REE geochemistry

Tables 1 and 2 present the rare earth element + yttrium geochemistry and data on the mineral chemistry of the granite, rhyolite and felsic dyke samples from the quarries of the study region respectively. Very high LREE, high

HREE, Sn, Hf and U contents are the hallmark of the present study. The chondrite-normalized REE patterns of the samples in this study showed a strong LREE enrichment (inclined pattern), a high HREE (flat pattern) and a highly fractionated pattern with a strong negative Eu anomaly (Figure 5 a). All the samples of granite, rhyolite and felsic dyke showed identical REE patterns indicating their crystallization from the same magma source. The multiple differentiation events that occurred in the source and possible late/post-magmatic metasomatic effects may have resulted in the variation in REE concentration in these rocks. The chondrite-normalized REE patterns of soil, loose gravel bed, oxidized zone and clay horizon showed similar REE trends as of granite, rhyolite and felsic dyke (Figure 5 b), confirming their *in situ* origin and occurring as weathered product.

REE mineralization in peralkaline igneous rocks is genetically related to the fractional crystallization of REE-rich magmatic fluid³⁸. However, REE mineralization in the studied samples is likely due to both magmatic and hydrothermal processes, resulting in an enrichment of REE concentration in the peralkaline host rock. This is demonstrated by the morphological characteristics, textural setting and chemical composition of the REE minerals observed in EPMA. The mineral chemistry of the major REE phases encountered during this study is discussed below.

Monazite

Monazite (La, Ce, Nd, Th) PO₄ is LREE-bearing phosphate and the most common REE-bearing mineral phase present. Monazite occurs as unzoned grain inclusions in arfvedsonite–aegirine, alkali feldspar and quartz. There are also large distinct monazite grains along the grain boundaries of arfvedsonite–aegirine and quartz, as well as aegirine–alkali feldspar (Figure 3 e and f). This REE phase contains Ce (33.96–34.50 wt% Ce₂O₃), La (21.63–25.68 wt% La₂O₃), Nd (6.41–9.66 wt% Nd₂O₃), Pr (3.02–3.47 wt% Pr₂O₃) and phosphate (28.67–29.79 wt% P₂O₅). The HREE occurrences in monazite are Sm (up to 1.14 wt% SmO) and Dy (up to 0.16 wt% Dy₂O₃). Monazite grains also contain Th (up to 0.26 wt% ThO₂) and minor amounts of Ca and Si.

Bastnaesite

Along the grain boundary of quartz–alkali feldspar, bastnaesite (Ce, La(CO)₃F) appears as a separate unique grain (20–50 µm) and as an inclusion inside quartz (Figure 3 f). It is dominated by Ce (29.30 wt% Ce₂O₃), La (12.07 wt% La₂O₃) and Nd (14.10 wt% Nd₂O₃), Pr (4.12 wt% Pr₂O₃) and F (2.65 wt%). The HREE contents in bastnaesite are Sm (3.16 wt% SmO), Gd (1.87 wt% Gd₂O₃), Dy (0.93 wt% Dy₂O₃) and Y (3.97 wt% Y₂O₃). Th (up to 0.13 wt% ThO₂), U (0.15 wt% UO₂) and small amounts of Si, Ca and Na are also present.

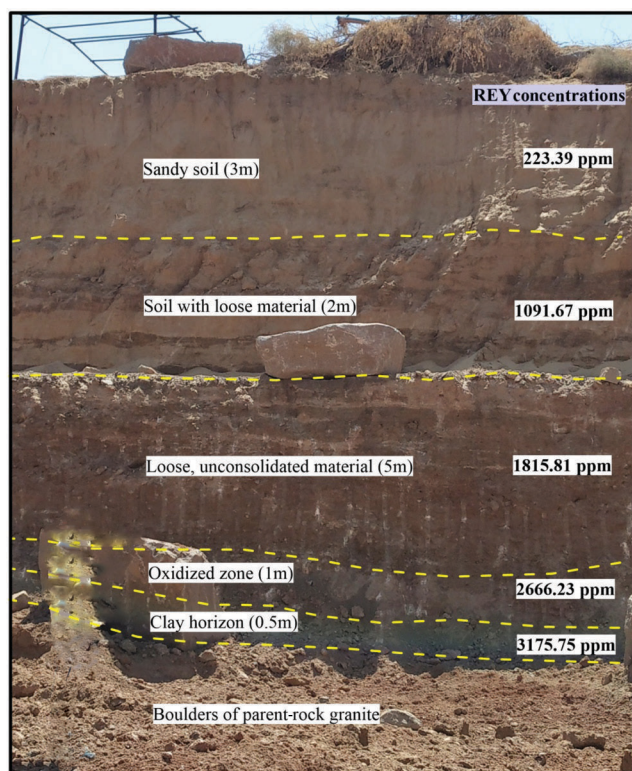


Figure 4. Soil profile exposed near Mawri area in one of the quarries and associated REE and Y concentration in different horizons.

Table 1. Representative EPMA analysis (wt%) of the studied samples from different quarries of the Siwana region

Oxide (wt%)	Silicate minerals						REE-bearing minerals					
	Aegirine	Arfvedsonite	Orthoclase	Albite	Perthite		Monazite	Bastnaesite	Zircon			
F	0.37	0.00	0.00	0.00	0.00	0.24	0.00	0.46	0.51	0.00	2.65	0.06
Na ₂ O	13.36	12.86	4.46	0.26	0.52	11.60	11.57	11.24	0.00	0.00	1.81	0.00
SiO ₂	52.91	53.02	49.10	64.25	64.64	69.30	69.87	70.70	0.51	0.53	20.58	39.70
MgO	0.04	0.00	0.10	0.01	0.01	0.02	0.00	0.04	0.01	0.00	0.00	0.00
Al ₂ O ₃	0.35	0.56	0.14	17.94	18.55	18.96	19.01	18.03	0.00	0.00	0.00	0.03
P ₂ O ₅	0.00	0.00	0.01	0.03	0.00	0.00	0.00	0.03	29.79	28.67	0.71	0.05
K ₂ O	0.00	0.51	0.02	16.47	16.08	0.13	0.16	0.29	0.01	0.00	0.01	0.00
CaO	0.17	0.07	13.95	0.00	0.00	0.02	0.01	0.02	0.01	0.06	3.81	16.93
TiO ₂	0.76	0.49	0.24	0.00	0.00	0.01	0.03	0.00	0.10	0.05	0.02	0.12
FeO	29.60	28.58	28.65	0.23	0.15	0.51	0.31	1.21	0.00	0.00	0.02	0.90
MnO	0.62	0.18	1.03	0.00	0.04	0.00	0.01	0.00	0.00	0.00	0.81	1.70
As ₂ O ₃	–	–	–	–	–	–	–	–	0.00	0.00	0.31	0.21
SrO	–	–	–	–	–	–	–	–	0.00	0.00	0.00	0.00
Nb ₂ O ₃	–	–	–	–	–	–	–	–	0.00	0.00	0.09	0.09
Y ₂ O ₃	–	–	–	–	–	–	–	–	0.00	0.00	3.97	0.31
BaO	–	–	–	–	–	–	–	–	0.00	0.01	0.00	0.32
La ₂ O ₃	–	–	–	–	–	–	–	–	21.63	25.67	12.07	0.00
Ce ₂ O ₃	–	–	–	–	–	–	–	–	33.96	34.50	29.30	0.00
Pr ₂ O ₃	–	–	–	–	–	–	–	–	3.47	3.02	4.12	0.14
Nd ₂ O ₃	–	–	–	–	–	–	–	–	9.66	6.41	14.10	0.00
SmO	–	–	–	–	–	–	–	–	1.14	0.01	3.16	0.07
Gd ₂ O ₃	–	–	–	–	–	–	–	–	0.08	0.00	1.87	0.00
Dy ₂ O ₃	–	–	–	–	–	–	–	–	0.16	0.00	0.93	0.00
WO ₃	–	–	–	–	–	–	–	–	0.30	0.00	0.21	0.00
UO ₂	–	–	–	–	–	–	–	–	0.00	0.02	0.15	0.00
PbO	–	–	–	–	–	–	–	–	0.00	0.03	0.00	0.00
ThO ₂	–	–	–	–	–	–	–	–	0.16	0.26	0.13	0.00
ZrO ₂	–	–	–	–	–	–	–	–	0.00	0.00	0.00	39.47
Cl	0.00	0.00	0.00	0.00	0.00	0.04	0.01	0.00	–	–	–	–
Cr ₂ O ₃	0.02	0.00	0.01	0.00	0.01	0.02	0.03	0.01	–	–	–	–
Total	98.18	96.27	97.71	99.19	100.00	100.84	101.00	102.04	101.48	99.25	100.84	100.09

Zircon

Zircon, Zr(SiO)₄ may contain U, Th, Pb, Hf, Y/REE and P. It occurs as separate grains as well as an inclusion within quartz. The grain size varies from 50 to 80 μm. It is dominated by Zr (39.47 wt% ZrO₂), Si (39.70 wt% SiO₂), Ca (16.93 wt% CaO), Y (0.31 wt% Y₂O₃) and Ba (0.32 wt% BaO) (Figure 3f).

Discussion

Peralkaline granite, rhyolite and felsic dykes of SRC belong to the Neoproterozoic MIS, which is a favourable geological province for hosting REE and rare metal (Sn, Hf) mineralization. The A-type Siwana peralkaline granite within the plate granite is characterized by high Na₂O + K₂O, Fe/Mg, Ga/Al, Mn, Zn, Ga, Zr, Nb and Y + REE, and low Al₂O₃, CaO, Sr and Ba^{35–37}. Mainly, two groups of REE minerals are identified, viz. REE-phosphate (monazite), REE-carbonate (bastnaesite), along with REE-bearing zircon. Table 3 shows the major REE minerals reported from SRC in the vicinity of studied quarries. The trace elements and REE geochemistry of studied rocks

from 17 quarries showed significant REE and Y. In granite, REE + Y value varied from 1061.26 to 5330.39 ppm with an average of 3014.97 ppm (*n* = 15), rhyolite showed REE + Y value between 1969.80 and 3148.97 ppm with an average of 2738.84 ppm (*n* = 4), and one of the felsic dykes showed REE + Y value of 9088.62 ppm. In all the studied samples (*n* = 20), LREE (La–Eu) ranged between 707.42 and 5743.83 ppm with an average of 2080.40 ppm, HREE (Gd–Lu) between 135.77 and 1422.23 ppm with an average of 402.41 ppm and Hf up to 425.55 ppm. The chondrite normalized REE pattern typically displayed enriched LREE, flat HREE pattern and strong negative Eu anomaly attributed to earlier fractionation of plagioclase in the parent magma. The LREE chondrite normalized values continuously decreased with increasing atomic number but remained constant in HREE. The average LREE to HREE ratio of known REE deposits in the world is 18 : 1, in comparison to 4.5 : 1 of the Siwana deposit.

The vertical distribution of REE and Y in the soil profile indicates a progressive depletion in the REE concentration from bottom to top. The clay horizon has the highest REE + Y concentration (3175.75 ppm) with an encouraging LREE/HREE ratio of 4.48 : 1. In contrast to REE pattern of the soil profiles from the tropical regions with a positive Ce

Table 2. REY and associated rare metal geochemistry of samples from different quarries of the Siwana region, Rajasthan, India

Sample ID	Rock types	La	Ce	Pr	Nd	Sm	Eu	Gd	Tb	Dy	Ho	Er	Tm	Yb
		All values are in ppm												
S-224/1	Granite	455.38	813.97	136.91	604.52	135.42	12.11	118.52	25.56	149.91	29.01	91.24	13.87	87.25
S-224/2	Granite	355.78	554.93	98.13	412.71	90.29	8.19	79.88	17.21	104.96	20.77	65.94	10.10	64.10
S-224/3	Granite	517.23	1025.76	176.72	766.42	179.27	15.93	157.17	34.63	213.74	42.54	131.24	19.67	118.72
S-224/4	Microgranite dyke	1018.65	2276.94	384.49	1641.26	387.56	34.92	327.83	70.22	411.23	79.42	232.49	37.45	231.39
S-228	Granite	241.25	447.05	66.05	290.30	59.61	5.83	55.09	10.89	63.99	12.41	38.25	5.82	38.92
VVK/26	Granite	306.61	680.33	87.14	391.74	91.44	8.21	76.92	16.51	106.04	21.10	65.06	9.52	60.36
VVK/63	Granite	139.60	329.10	38.77	159.97	35.65	4.33	28.53	6.26	39.18	7.85	23.80	3.44	23.28
VVK/78	Granite	337.52	677.67	90.03	385.68	89.39	9.52	83.59	16.87	103.55	20.12	61.15	8.98	52.65
VVK/110	Granite	410.62	1045.00	103.35	461.42	101.97	9.17	84.25	19.47	124.01	24.82	79.27	12.22	73.39
VVK/146	Rhyolite	470.39	979.00	122.91	465.93	91.11	10.18	83.38	17.39	106.69	20.96	64.42	9.84	61.58
VVK/220	Granite	614.86	1407.12	97.41	404.69	84.98	6.73	76.44	15.65	96.06	18.69	57.49	8.93	53.92
VVK/232	Granite	428.28	931.27	67.73	288.94	60.41	5.07	54.43	10.93	65.35	12.51	37.80	5.85	35.58
VVK/235	Granite	455.47	1088.72	68.43	281.03	59.49	4.79	54.59	11.44	70.09	13.76	42.11	6.62	40.11
VVK/248	Granite	348.61	705.62	50.33	213.20	46.60	4.54	41.95	8.92	52.92	10.41	32.46	5.00	32.05
VVK/249	Granite	633.55	1359.17	95.90	401.40	89.98	8.56	82.89	18.51	118.73	23.91	77.66	12.34	76.85
VVK/267	Granite	595.13	1300.14	154.35	578.58	152.33	14.37	147.53	33.01	200.86	39.96	121.50	18.21	110.47
VVK/291	Rhyolite	351.85	670.02	51.83	215.95	45.56	5.92	39.60	8.18	48.16	9.17	28.04	4.33	27.12
VVK/241	Rhyolite	454.59	960.93	66.52	276.21	56.81	6.02	47.80	9.76	60.45	12.32	38.37	6.17	38.66
VVK146	Rhyolite	470.39	979.00	122.91	465.93	91.11	10.18	83.38	17.39	106.69	20.96	64.42	9.84	61.58
VVK/208	Granite	449.97	973.69	69.50	291.33	61.90	4.92	55.63	11.45	68.83	13.44	41.46	6.55	39.94
S-224/5	Sandy soil	37.29	71.98	8.80	36.06	7.32	1.14	6.19	1.18	6.57	1.31	3.93	0.60	3.63
S-224/6	Loose gravel	152.96	335.43	39.81	169.39	35.68	3.81	31.81	6.49	39.40	7.78	23.73	3.82	22.93
S-224/7	Loose gravel	278.20	442.97	75.32	321.57	68.56	6.26	61.37	12.76	78.56	15.72	47.77	7.59	45.38
S-224/8	Oxidized zone	346.08	558.43	94.43	404.01	84.80	7.72	76.24	16.33	101.32	19.73	62.73	9.98	61.64
S-224/9	Clay horizon	415.26	836.09	144.32	608.46	122.68	10.38	108.93	22.48	134.15	26.39	82.01	12.78	78.70

Sample ID	Rock types	Lu	Y	Be	Ge	Mo	Sn	Hf	Ta	W	U	LREE (La–Eu)	HREE (Gd–Lu)	REY
		All values are in ppm												
S-224/1	Granite	12.49	646.79	37.95	3.44	10.72	53.66	167.98	11.02	3.50	16.63	2158.30	527.85	3332.94
S-224/2	Granite	9.30	506.14	29.30	3.12	4.51	49.20	123.99	5.44	76.77	14.75	1520.03	372.25	2398.43
S-224/3	Granite	16.19	930.81	50.11	4.24	5.16	61.61	192.68	16.13	6.00	25.94	2681.32	733.90	4346.03
S-224/4	Microgranite dyke	32.20	1922.57	35.72	5.37	10.65	84.98	296.43	28.91	38.73	22.79	5743.83	1422.23	9088.62
S-228	Granite	5.42	358.74	20.65	2.86	6.02	32.47	113.80	2.59	1.39	9.58	1110.09	230.79	1699.62
VVK/26	Granite	8.54	570.48	21.85	2.89	5.58	29.55	83.07	14.47	18.89	9.87	1565.47	364.04	2499.99
VVK/63	Granite	3.44	218.07	11.75	2.09	0.66	94.24	41.12	4.67	<0.50	4.10	707.42	135.77	1061.26
VVK/78	Granite	6.94	570.64	22.51	2.36	1.72	43.18	124.04	12.75	3.19	10.51	1589.81	353.85	2514.31
VVK/110	Granite	10.35	775.05	37.08	2.82	4.56	37.42	96.64	2.69	9.94	15.12	2131.52	427.76	3334.33
VVK/146	Rhyolite	8.74	636.45	25.83	1.85	1.12	51.31	166.11	10.75	5.50	16.22	2139.51	373.00	3148.97
VVK/220	Granite	7.41	978.16	29.45	3.21	4.09	78.58	117.98	15.87	13.17	10.73	2615.78	334.59	3928.53
VVK/232	Granite	5.01	658.49	17.65	3.68	7.08	37.54	94.40	4.08	6.64	7.86	1781.71	227.46	2667.66
VVK/235	Granite	5.72	741.51	22.72	2.70	4.35	37.55	97.71	5.86	13.44	9.44	1957.92	244.44	2943.86
VVK/248	Granite	4.68	547.32	15.47	2.44	7.71	48.21	49.35	7.14	3.95	6.90	1368.89	188.40	2104.61
VVK/249	Granite	10.06	1283.57	23.97	3.28	7.47	72.61	144.16	20.37	8.84	16.47	2588.55	420.95	4293.07
VVK/267	Granite	15.66	1848.30	14.58	3.66	10.09	48.97	425.55	19.04	13.70	15.17	2794.89	687.20	5330.39
VVK/291	Rhyolite	3.89	450.18	14.35	1.93	5.22	45.42	70.36	4.66	<0.5	4.65	1341.13	168.49	1959.80
VVK/241	Rhyolite	5.60	626.68	30.20	3.21	1.77	41.19	117.75	4.48	5.17	7.82	1821.08	219.14	2666.89
VVK146	Rhyolite	8.74	636.45	25.83	1.85	1.12	51.31	166.11	10.75	5.50	16.22	2139.51	373.00	3148.97
VVK/208	Granite	5.76	675.23	26.39	2.96	3.88	37.80	116.56	6.96	6.48	9.15	1851.32	243.05	2769.60
S-224/5	Sandy soil	0.54	36.85	3.16	1.15	2.97	2.14	8.46	1.00	1.31	1.74	162.59	23.94	223.39
S-224/6	Loose gravel	3.31	215.33	11.46	1.94	1.74	18.18	50.28	1.38	28.22	5.48	737.08	139.26	1091.67
S-224/7	Loose gravel	6.55	347.23	19.71	2.67	2.55	31.84	84.94	5.27	2.40	9.83	1192.88	275.71	1815.81
S-224/8	Oxidized zone	9.00	413.78	30.11	2.76	3.82	48.26	109.78	8.71	42.55	13.17	1495.48	356.98	2266.23
S-224/9	Clay horizon	11.34	561.78	41.45	3.48	7.84	52.18	143.26	11.57	10.69	17.35	2137.19	476.77	3175.75

anomaly, where Ce^{3+} is readily oxidized to Ce^{4+} and gets precipitated along with Fe/Mn (oxy)hydroxides, the samples from Siwana exhibited weak negative Ce anomaly along with strong negative Eu anomaly akin to the chondrite normalized REE pattern of bedrock samples. The

vertical distribution of REE and Y indicated a progressive depletion in the REE concentration from bottom to top. The similarity of the REE pattern of all soil profile samples with the bedrock samples suggests low mobility of REE during the weathering process.

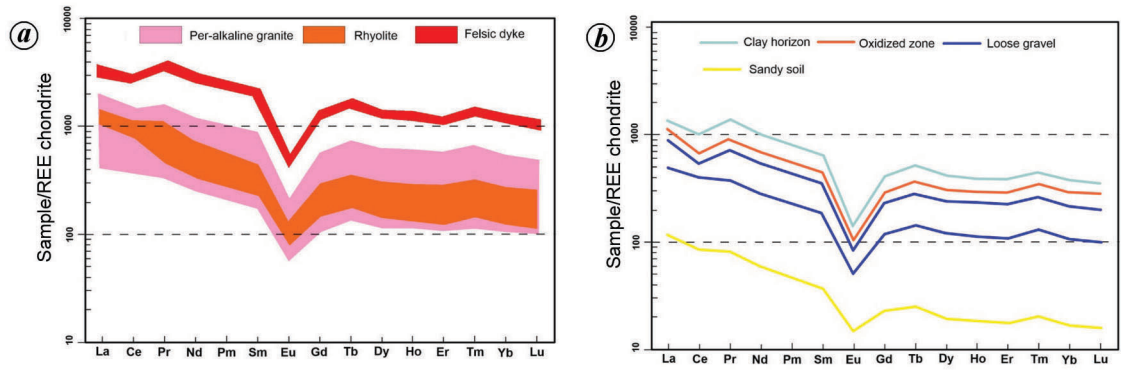


Figure 5. Chondrite-normalized REE pattern of (a) peralkaline granite, rhyolite and felsic dyke and (b) sandy soil, loose gravel, oxidized zone and clay horizon from building stone quarries in the present study (after Nakamura⁴³).

Table 3. Major REE mineral phases reported from different parts of the Siwana Ring Complex

REE phosphate	REE carbonate	REE silicate	REE oxide/hydroxide	Reference
Monazite	Bastnasite, parasite, galgenbergite	Allanite, chevkinite, zircon, gittinsite	Aeshynite, ceriopyrochlore, Th-bearing thorosteenstrupine	44
Monazite	Parasite	Eudialyte, perrierite, tritomite, zircon	–	11, 12
Xenotime, monazite	Bastnasite (La–Ce), parasite, La–Ce–Ba cebaite, carbocernaite, ancylite, strontianite	Zircon, allanite	Cerianite, thorianite, celestire, fergusonite	13
Fluorapatite, monazite, apatite	Parasite, bastnäsité–Ce	Eudialyte	Cerite, vlasovite, chevkinite–Ce	45

The origin of high field strength elements and REE mineralization associated with peralkaline rocks is uncertain, and there is debate as to mineralization, i.e. magmatic, hydrothermal or a combination of both^{38–42}. The alkaline nature of magmatism in the study area suggests the possibility of an essentially REE-enriched magmatic source. The magmatic model assumes that REE got enriched due to prolonged fractional crystallization. The REE enrichment levels in various magmatic phases, rhyolite, granite and felsic dykes in the order of abundance, can be the result of a protracted fractionation of an REE-rich source. The petrographic study reveals the presence of primary (magmatic) REE-bearing mineral phases within the REE-hosted litho units. The magmatic REE-bearing phases such as monazite (phosphate), allanite (silicate) and zircon are distributed as well-preserved euhedral grains and as inclusions in other magmatic phases. The ubiquitous presence of well-preserved magmatic monazites confirms the availability of phosphate-rich melts in the source.

However, mineralization is associated with altered parts of alkaline intrusion in a number of world-class deposits, suggesting enrichment due to hydrothermal activity. The anhedral secondary REE-bearing mineral grains are mostly distributed along the grain boundaries and as intrusions to the primary minerals. The REE carbonates (Bastneasite), zirconium silicate, and apatite are major secondary REE-bearing phases that most likely evolved from an event of hydrothermal activity. A post-/late-magmatic hydrother-

mal event is well evident in granite under the microscope as coarsening of perthite lamellae, pseudomorphic replacement of alkali feldspar grains by aegirine, and replacement of aenigmatite by aegirine. Therefore, both magmatic and hydrothermal events likely contributed to the formation of REE-enriched peralkaline felsic rocks in the study area.

Concluding remarks

The peralkaline felsic rocks of SRC are a source of concentrated REE (both LREE and HREE) and Y. Maximum concentration was reported from the younger derivatives, viz. felsic dykes such as rhyolite, microgranite, aplite and felsite dykes. The vertical distribution of REE and Y in the studied soil profile indicates a progressive depletion in the REE concentration from bottom to top due to the low mobility of REE during the weathering process. The present study reveals that REE and Y mineralization in the rocks of SRC is essentially magmatic. A late to post-magmatic redistribution of REE, Y and RM is an unambiguous reality.

1. GoI, Mining of rare earth elements, Department of Atomic Energy, Government of India, Press release, 2023; <https://www.pib.gov.in/PressReleasePage.aspx?PRID=1914305>.
2. Hoatson, D. M., Jaireth, S. and Mieztis, Y., The major rare-earth-element deposits of Australia: geological setting, exploration and resources. Geoscience Australia, Canberra, 2011, p. 204.
3. Long, K. R., Gosen, B. S. V., Foley, N. K. and Cordier, D., The principal rare earth elements deposits of the United States – a

- summary of domestic deposits and a global perspective. US Geological Survey Scientific Investigations Report, 2010, SIR 2010–5220, p. 96; <http://pubs.usgs.gov/sir/2010/5220/>
4. Varughese, S. K., Banerjee, A., Kamlesh, K., Bidwai, R., Sarbajna, C., Bhatt, A. K. and Verma, M. B., Field setting, mineralogy, geochemistry, and potential of acid volcanics hosting REE–Nb–Zr ± U mineralisation in Siwana ring complex, Barmer district, Rajasthan. In Proceedings of National Seminar on Strategic Mineral Exploration for Sustainable Development: Emerging Trends and Challenges, Atomic Minerals Directorate for Exploration and Research, Southern Region, Bengaluru, 7–8 May 2019, abstr. vol., pp. 92–93.
 5. Banerjee, A. *et al.*, Geology and geochemistry of peralkaline acid volcanic-hosted REE–Nb occurrence in Dantala area, Siwana Ring Complex, Barmer district, Rajasthan. In Proceedings of the International Seminar Carbonatites–Alkaline Rocks and Associated Mineral Deposits (eds Viladkar, S. G., Duraiswami, R. A. and Krishnamurthy, P.), Amba Dongar, Gujarat, 2017, abstr. vol., p. 45.
 6. Padhi, A. K., Paul, A. K., Mundra, K. L., Pandey, K. K., Sunil, K., Hamilton, S. and Verma, M. B., Electron microprobe analyses of REE-bearing phases in microgranite, Nal area, Siwana Ring Complex, Rajasthan. In Proceedings of National Seminar on Strategic Mineral Exploration for Sustainable Development: Emerging Trends and Challenges, Atomic Minerals Directorate for Exploration and Research, Southern Region, Bengaluru, 2019, abstr. vol. 77.
 7. Bidwai, R., Srinivasan, S., Nanda, L. K., Banerjee, A., Bangroo, P. N., Rai, A. K. and Parihar, P. S., Anomalous silver concentration in volcano-plutonic rocks of Siwana Ring Complex, Barmer district, western Rajasthan. *Curr. Sci.*, 2014, **106**, 159–162.
 8. Balram, V., Rare earth elements: a review of applications, occurrence, exploration, analysis, recycling, and environmental impact. *Geosci. Fron.*, 2019, **10**, 1285–1303; <https://doi.org/10.1016/j.gsf.2018.12.005>.
 9. Zepf, V., Rare earth elements: what and where they are. In *Rare Earth Elements*, Springer, Berlin, Heidelberg, 2013; https://doi.org/10.1007/978-3-642-35458-8_2.
 10. Cook, N. J., Ciobanu, C. L., Meria, D., Silcock, D. and Wade, B., Arsenopyrite–pyrite association in an orogenic gold ore: tracing mineralization history from textures and trace elements. *Econ. Geol.*, 2013, **108**(6), 1273–1283.
 11. Das, U. K., Ghantait, A., Panda, L. and Hussain, S., Rare earth element potential of the felsite dykes of Phulan area, Siwana Ring Complex, Rajasthan, India. *Curr. Sci.*, 2016, **110**(7), 1157–1162.
 12. Das, U. K. and Gantait, A., REE mineral chemistry and the nature of REE mineralization: a study from felsite dykes of Phulan area, Siwana Ring Complex, Rajasthan, India. *J. Earth Syst. Sci.*, 2020, **129**(1), 1–18.
 13. Bhushan, S. K. and Somani, O. P., Rare earth elements and yttrium potentials of Neoproterozoic peralkaline Siwana granite of Malani igneous suite, Barmer district, Rajasthan. *J. Geol. Soc. India*, 2019, **94**(1), 35–41.
 14. Bhushan, S. K., Late Proterozoic continental growth: implications from geochemistry of acid magmatic events of west Indian craton, Rajasthan. *Geol. Soc. India Mem.*, 1995, **34**, 339–355.
 15. Choudhary, A. K., Gopalan, K. and Sastry, C. A., Present status of the geochronology of the Precambrian rocks of Rajasthan. *Tectonophysics*, 1984, **105**, 131–140.
 16. Bhushan, S. K., Neoproterozoic magmatism of the Malani Igneous Suite, western Rajasthan, India. *Geol. Surv. India, Spec. Publ.*, 2000, **55**, 319–332.
 17. Singh, A. K. and Vallinayagam, G., Radioactive element distribution and rare-metal mineralization in anorogenic acid volcano-plutonic rocks of the Neoproterozoic Malani felsic province, western peninsular India. *J. Geol. Soc. India*, 2009, **73**, 837–853.
 18. Singh, L. S. and Vallinayagam, G., Geochemistry and petrogenesis of acid volcanoplutonic rocks of the Siner area, Siwana Ring Complex, northwestern Peninsular India. *J. Geol. Soc. India*, 2013, **82**(1), 67–79.
 19. Kochhar, N., Mineralization associated with A-type Malani magmatism, northwestern peninsular India. In *Metallogeny Related to Tectonics of the Proterozoic Mobile Belts* (ed. Sarkar, S. C.), Oxford IBH, New Delhi, 1992, pp. 209–224.
 20. Kochhar, N., Attributes and significance of the A-type Malani magmatism, northwestern peninsular India; In *Crustal Evolution and Metallogeny in the Northwestern India Shield* (ed. Deb, M.), Narosa Publishers, New Delhi, 2000, pp. 158–188.
 21. Jain, R. B., Miglani, T. S., Kumar, S., Swarnkat, B. M. and Singh, R., Rare metal and rare earth rich peralkaline, agpaiticgranitoid dykes of Siwana Ring Complex, District Barmer, Rajasthan. *Curr. Sci.*, 1996, **70**, 854–858.
 22. Bhushan, S. K. and Chittora, V. K., Late Proterozoic bimodal assemblage of Siwana subsidence structure, western Rajasthan, India. *J. Geol. Soc. India*, 1999, **53**, 433–453.
 23. Vallinayagam, G., Geochemistry and petrogenesis of basic rocks in the Siwana ring complex, Barmer district, Rajasthan, India. *Indian Miner.*, 2001, **35**, 121–133.
 24. Vallinayagam, G., A report on rare metals and rare earths in the Siwana ring complex, Rajasthan. *J. Appl. Geochem.*, 2004, **6**(2), 387–391.
 25. Vallinayagam, G. and Kochhar, N., Geochemical characteristic and petrogenesis of A-type granite and the associated acid volcanic of the Siwana ring complex, northern peninsular, India. In *The Indian Precambrian* (ed. Paliwal, B. S.), Scientific Publisher, Jodhpur, 1998, pp. 460–481.
 26. Bhushan, S. K. and Mohanty, M., Mechanics of intrusion and geochemistry of alkaline granites from Siwana, Barmer district, Rajasthan. *Indian J. Earth Sci.*, 1988, **15**, 103–115.
 27. Gong, Q., Deng, J., Yang, L., Zhang, J., Wang, Q. and Zhang, G., Behavior of major and trace elements during weathering of sericite – quartz schist. *J. Asian Earth Sci.*, 2011, **42**, 1–13.
 28. Öhlander, B., Land, M., Ingri, J. and Widerlund, A., Mobility of rare earth elements during weathering of till in northern Sweden. *Appl. Geochem.*, 1996, **11**, 93–99.
 29. Kissao, G. and Heinz, J. T., Distribution patterns of rare-earth elements and uranium in tertiary sedimentary phosphorites of Hahotoé–Kpogamé, Togo. *J. Afr. Earth Sci.*, 2003, **37**, 1–10.
 30. Laveuf, C. and Cornu, S., A review on the potentiality of rare earth elements to trace pedogenetic processes. *Geoderma*, 2009, **154**, 1–12.
 31. Babechuk, M. G., Widdowson, M. and Kamber, B. S., Quantifying chemical weathering intensity and trace element release from two contrasting basalt profiles, Deccan Traps, India. *Chem. Geol.*, 2014, **363**, 56–75.
 32. Ndjigui, P. D., Bilong, P., Bitom, D. and Dia, A., Mobilization and redistribution of major and trace elements in two weathering profiles developed on serpentinites in the Lomié ultramafic complex, South-East Cameroon. *J. Afr. Earth Sci.*, 2008, **50**, 305–328.
 33. Lee, S., Lee, D., Kim, Y., Chae, B., Kim, W. and Woo, N., Rare earth elements as indicators of groundwater environment changes in a fractured rock system: evidence from fracture-filling calcite. *Appl. Geochem.*, 2003, **18**, 135–143.
 34. Liu, F., Miao, L., Cai, G. and Yan, W., The rare earth element geochemistry of surface sediments in four transects in the South China Sea and its geological significance. *Environ. Earth Sci.*, 2015, **74**, 2511–2522.
 35. Eby, G. N. and Kochhar, N., Geochemistry and petrogenesis of the Malani Igneous Suite, northern India. *J. Geol. Soc. India*, 1990, **36**, 109–130.
 36. Maheshwari, A., Sial, A. N., Coltorti, M., Chittora, V. K. and Cruz, M. J. M., Geochemistry and petrogenesis of Siwana peralkaline granites, West of Barmer, Rajasthan, India. *Gondwana Res.*, 2001, **4**(1), 87–95.
 37. Mohanty, M. and Bhushan, S. K., Neoproterozoic peralkaline Siwana granite, Barmer district, Rajasthan and its potential for rare earth element mineralization. *Geol. Surv. India, Spec. Publ.*, 2004, **72**, 363–376.

38. Salvi, S. and Williams-Jones, A. E., The role of hydrothermal processes in the granite-hosted Zr, Y, REE deposits at Strange Lake, Quebec/Labrador: evidence from fluid inclusion: *Geochim. Cosmochim. Acta*, 1990, **54**, 2403–2418.
39. Dostal, J., Chatterjee, A. K. and Kontak, D. J., Chemical and isotopic (Pd, Sr) zonation in a peraluminous granite pluton: role of fluid fractionation. *Contrib. Mineral. Petrol.*, 2004, **147**, 74–90.
40. Halter, W. and Webster, J. D., The magmatic to hydrothermal transition and its bearing on ore-forming systems. *Chem. Geol.*, 2004, **210**, 1–6.
41. Veksler, I. V., Liquid immiscibility and its role at the magmatic hydrothermal transition: a summary of experimental studies: *Chem. Geol.*, 2004, **210**, 7–31.
42. Linen, R. L. and Cuney, M., Granite-related rare-element deposits and experimental constraints on Ta–Nb–W–Sn–Zr–Hf mineralization. Geological Association of Canada short course notes, 2005, vol. 17, pp. 45–68.
43. Nakamura, N., Determination of REE, Ba, Fe, Mg, Na and K in carbonaceous and ordinary chondrite. *Geochim. Cosmochim. Acta*, 1974, **38**, 757–775.
44. Rastogi, S. K., Mukherjee, T. and Gupta, G. P., Flow stratigraphy, geochemistry and REE mineralization in northern part of the Siwana Ring Complex in Malanilgeneous Suite (MIS), Barmer district, Rajasthan. Recent development in metallogeny and mineral exploration in Rajasthan. *Geol. Surv. India, Spec. Publ.*, 2015, **101**, 207–217.
45. Mondal, S., Upadhyay, D. and Banerjee, A., REE mineralization in Siwanaperalkaline granite, western India – role of fractional crystallization, hydrothermal remobilization, and feldspar-fluid interaction. *Lithos*, 2021, **396–397**, 106240.

ACKNOWLEDGEMENTS. We thank the Additional Director General and Head, Geological Survey of India (GSI), Western Region (WR), Jaipur, for logistics support and the Deputy Director General and RMH-II (GSI, WR) for the technical support while carrying out this work. We also thank Shri Suresh Chander (Director, GSI, WR) and Shri Rohan Das (Director GSI, WR), for support; the anonymous reviewers for their useful suggestions, and the Regional Chemical Laboratory (GSI, WR) and EPMA Laboratory, Faridabad for help with analysis of EPMA samples.

Received 22 March 2023; re-revised accepted 25 December 2023

doi: 10.18520/cs/v126/i5/583-592
